ResearchGate

See discussions, stats, and author profiles for this publication at: https://www.researchgate.net/publication/247778451

Ettringite Strengthening at High Pressures Induced by the 2 Densification of the Hydrogen Bond Network

ARTICLE *in* THE JOURNAL OF PHYSICAL CHEMISTRY C · JANUARY 2013

Impact Factor: 4.77 · DOI: 10.1021/jp301822e

CITATIONS
6

READS
45

5 AUTHORS, INCLUDING:

Hegoi Manzano
Universidad del País Vasco / Euskal Herriko …
41 PUBLICATIONS **479** CITATIONS
SEE PROFILE

A. Ayuela
Universidad del País Vasco / Euskal Herriko …
130 PUBLICATIONS **2,718** CITATIONS
SEE PROFILE

P. J. M. Monteiro
University of California, Berkeley
285 PUBLICATIONS **4,028** CITATIONS
SEE PROFILE

J.s. Dolado
Tecnalia
57 PUBLICATIONS **1,090** CITATIONS
SEE PROFILE

Available from: Hegoi Manzano
Retrieved on: 02 February 2016

THE JOURNAL OF PHYSICAL CHEMISTRY C

Article

pubs.acs.org/JPCC

Ettringite Strengthening at High Pressures Induced by the Densification of the Hydrogen Bond Network

H. Manzano,*[,†,‡] A. Ayuela,[§] A. Telesca,[∥] P. J. M. Monteiro,[⊥] and J. S. Dolado[#]

[†]Molecular Spectroscopy Laboratory, Physical Chemistry Department, UPV/EHU, 48940 Leioa, Spain

[‡]Concrete Sustainability Hub, Civil and Environmental Engineering Department, Massachusetts Institute of Technology, Cambridge MA02139, United States

[§]Departamento de Física de Materiales, Facultad de Químicas, Centro de Física de Materiales CSIC-UPV/EHU and Donostia Internacional Physics Center, 20018, San Sebastián/Donostia, Spain

[∥]Dipartimento di Ingegneria e Fisica dell'Ambiente, Università degli Studi della Basilicata, Contrada Macchia Romana, 85100 Potenza, Italy

[⊥]Department of Civil and Environmetal Engineering, University of California, Berkeley, California 94720, United States

[#]TECNALIA Research & Innovation, Parque Tecnológico de Bizkaia Edificio 700, 48160, Derio, Spain

ABSTRACT: Ettringite is a rare mineral with high-water content, more than half of its weight, and a relevant secondary product in Portland cement. Using density functional theory, we simulate the crystal structure and properties of ettringite under pressure. Our calculations predict a change in slope for all the lattice parameters versus pressure at about 2.5 GPa. Above such pressure, the elastic properties show a drastic increase of nearly 80% in the bulk modulus. This finding is explained in terms of a concurrent amorphization and densification of the hydrogen bond network. At low pressures, ettringite can be compressed substantially without significant repulsion in the hydrogen bond network. At high pressures, the hydrogen bonds become stiff, and their contribution to the total repulsion is then important. These changes are also supported by the evolution on the electronic density of ettringite with pressure.

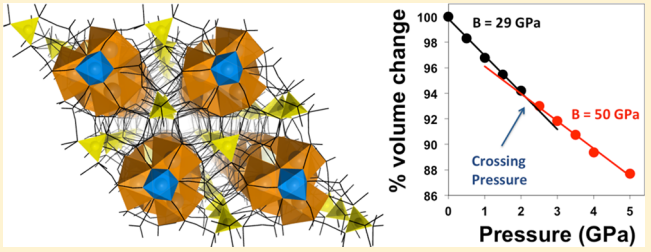

INTRODUCTION

Ettringite is a mineral that forms near igneous contacts or in xenoliths environments, associated with other species like portlandite, gypsum or afwillite.[1] Ettringite crystals are hexagonal with a symmetry group $P31c$ and a molecular formula of $Ca_6Al_2(SO_4)_3(OH)_{12}\cdot nH_2O$ (n = 24−27). Its high water content, more than one-half of its mass, confers to ettringite a low density of approximately 1.745 g·cm^{-3}. The unit cell structure, shown in Figure 1, is based on calcium aluminate columns aligned here parallel to the c-axis. Along the column, the aluminum atoms are octahedrally coordinated to hydroxyl groups and intercalated between planes with three calcium atoms. The Ca atoms are coordinated to the hydroxyl groups of aluminum and to four water molecules. The stoichiometry of the columns leads to a charge excess, which is neutralized by sulfate ions located in the channels between these columns. Several experiments by X-ray diffraction reported that the space between columns is filled with a variable number of water molecules.[2−7]

Experimental works on ettringite have clearly pointed to the important role of water molecules in the cohesion between columns. Moore and Taylor, when first resolving the crystalline structure of ettringite, suggested that the water molecules transfer the charge from the calcium-aluminate to the negative sulfate ions giving cohesion to the crystal.[8] Ettringite can lose about 27% of its structural water, including some of the hydroxyl group when it is heated up to 50 °C.[3] If the thermal treatment continues and 30% of the water is lost, the crystalline

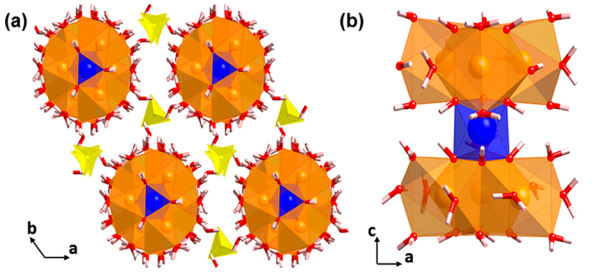

Figure 1. (a) Crystal structure of ettringite viewed along the c axis direction. Aluminate ions (AlO_3^{3-}) are shown as blue octahedra, sulfate ions (SO_4^{2-}) are shown as yellow tetrahedra, and calcium ions are inside orange polyhedra. Water and hydroxyl groups are denoted with red and white sticks for O and H atoms, respectively. (b) Detail of a calcium-aluminate column.

Received: February 23, 2012
Revised: June 28, 2012

 © XXXX American Chemical Society dx.doi.org/10.1021/jp301822e | J. Phys. Chem. C XXXX, XXX, XXX−XXX

order disappears,[3] a process that suggests a strong role of water in its structural integrity ettringite. The high water content of ettringite also affects its elastic properties. Using Brioullin spectroscopy,[2] the elastic moduli along the *c* direction was found to be larger than in the *ab* plane by nearly a factor of 2. Such anisotropy is attributed to the stiffer iono-covalent bonds in the calcium-aluminate columns compared to the electrostatic bonding mediated by water in the ab plane.[2] These experimental studies revised so far indicate the basic role of water, which must be carefully studied when looking at the bonding and the elastic properties of ettringite.

The technological interest of ettringite arises from its presence in the hydration of Portland cement. Ettringite forms as a hydration product of calcium aluminate phases and gypsum, and it establishes a complex equilibrium with other crystalline phases in cement, such as monosulphoaluminate.[9] During the early hydration, ettringite crystals played an important role in the cement setting and workability of cements, and their presence must be carefully controlled.[9,10] At later ages, ettringite might form in concrete under humid environments owing to sulfate attack. As a result of the crystallization pressure and water adsorption, this secondary formation of ettringite often causes microcracks in cement pastes, which reduce their performance.[11] Ettringite is also the main binding phase of calcium sulphoaluminate cements, a more environmentally friendly alternative to ordinary cement, and a current focus in scientific and technological research.[12] Another potential application of ettringite is waste management.[13] Oxyanions such as $B(OH)^{4-}$, SeO_4^{2-}, CrO_4^{2-}, and MoO_4^{2-} can be stabilized in the channels between columns, occupying the position of the sulfate groups.[14] Divalent and trivalent metals can compete with aluminum for the octahedral positions within the columns, and ettringite with Cu, Cr, Cd, Fe, Pb, and Zn substitutions have been synthesized.[15]

The practical manufacturing of cement-based materials and the efficient stabilization of heavy ions require that we are able to understand and control the properties of ettringite under a wide range of thermodynamic conditions, such as high pressures. Despite the fact that the effect of temperature on the stability of ettringite has been studied in depth, just one article reported the structural changes as the pressure increases.[6] In that work, the authors determined that at a pressure of 3 GPa, ettringite lost the long-range crystalline order because its X-ray diffraction pattern showed a broad reflection instead of defined peaks. The recovery of crystalline order when pressure decreases suggests that water does not leach in the process.[6] Measured by IR spectroscopy, the O−H and S−O vibrational bands suggest an amorphization of the water network, preserving the basic structure of ettringite.

In this work we aim to further understand the structure and properties of ettringite with or without pressure using density functional theory (DFT) simulations. We analyzed the atomic structure and electronic properties up to 5 GPa. Special attention was paid to the changes on the water network, which we will show is indeed the critical factor that drives the singular behavior of ettringite crystals under pressure. Due to the high-water content, ettringite serves as a model to study the impact of water in the structure and properties of inorganic crystals.

COMPUTATIONAL DETAILS

The simulations were carried out in the framework of the DFT, as implemented in the SIESTA code.[16] The exchange-correlation functional was chosen from the generalized gradient approximation (GGA)[17] following the Perdew−Burke−Ernzerhof (PBE) scheme.[18] SIESTA is based on a combination of the localized atomic orbitals basis set and pseudopotentials to perform calculations of the electronic structure. The pseudopotentials and double zeta polarized (DZP) basis sets for Al−Ca−O−H were tested previously,[19−21] which showed an excellent agreement with the experimental crystalline structures and elastic properties of calcium aluminates. We considered a $3s^2\ 3p^4$ atomic configuration for sulfur atoms using a DZP basis set. The converged simulations were done using a mesh cutoff of 350 Ry and several k-points given by the grid cutoff of 10.78 Å.[22] The unit cell is relaxed by the conjugate gradient method simultaneously minimizing the atomic positions and the lattice parameters. The convergence criterion for the atomic forces is 0.02 eV·Å^{-1}. The pressure was applied isotropically to the unit crystalline cell. The elastic tensor coefficients were finally calculated from the strain−stress relationship. The strains were applied in steps of 0.5% from −3% to +3% to calculate the corresponding stresses, so that after a linear fit, the elastic coefficients are obtained.

RESULTS AND DISCUSSION

We first looked at the effect of different water amounts on the structure of ettringite, since they partially occupy the empty spaces in the intercolumn channels.[2−7] We have analyzed the crystalline structure of ettringite for the whole range of possible water occupancies in the unit cell, from 24 to 27. Table 1 collects our computed lattice parameters. The increase from 24 to 27 water molecules in the ettringite unit cell has a small effect on its lattice parameters. The lattice constants *a* and *b* increase by 1%, and the change in the *c* dimension remains small within 0.25%. This results in a maximum cell volume increase of 2.3%. Although our lattice constants are slightly larger than the experimental data, also given in Table 1, they still agree well.

Table 1. Lattice Parameters of Ettringite from Our Calculations and Experimental Values from the Literature

structure	*a*−*b* (Å)	*c* (Å)	volume (Å)	density (g/cm^3)	water
this work	11.217	21.575	2357.90	1.717	24
	11.241	21.604	2364.15	1.737	25
	11.289	21.617	2385.57	1.747	26
	11.338	21.6437	2411.86	1.753	27
ICDD 41-1451	11.224	21.408	2335.62	1.79	26
Speziale[2]	11.24	21.468	2348.80	1.78	26
Hartman[3]*	11.116	21.355	2285.22	1.81	25
Berliner[7]*	1.117	21.360	2306.81	1.90	26
Taylor[4]	11.260	21.48	2358.53	1.76	25.7
Neubauer[5]*	11.229	21.478	2345.46	1.77	25.7
Clark[6]	11.240	21.468	2348.80	1.78	26

Figure 2 shows a simulated X-ray powder diffraction pattern of ettringite structure with 26 water molecules in the unit cell, together with the experimental spectrum generated after the recent data reported by Hartman and Berliner.[23] Note the excellent match in the position and intensity of the peaks, just slightly shifted to larger *d*-spacing due to the increase of the lattice dimensions. This match ensures that the atomic arrangement and structural features are fully conserved after relaxation. Also of interest is the presence of a small peak at 7.3 Å. It has been suggested that such peak might arise from

dx.doi.org/10.1021/jp301822e | J. Phys. Chem. C XXXX, XXX, XXX−XXX

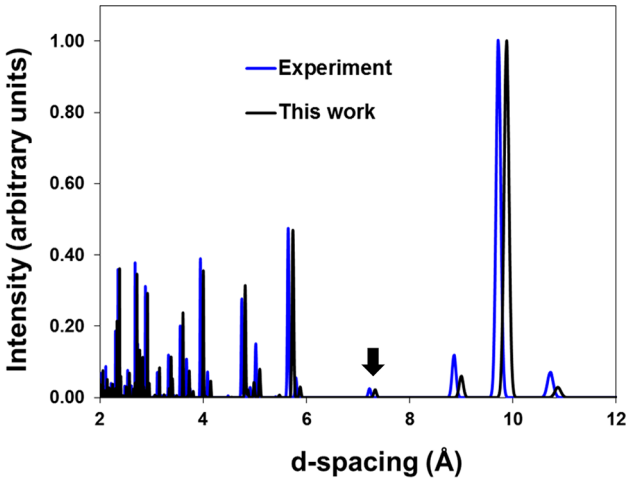

Figure 2. X-ray powder diffraction patterns of ettringite obtained from the computed structure using the Mercury code[24] (black) and from experiments[23] (blue).

impurities in the sample.[6] However, its presence in our simulated X-ray diffraction pattern shows that the peak is intrinsic to the ettringite structure and independent of impurities.

Our simulations accurately described the unit cell and atomic arrangement of ettringite, and we have determined that the variation in stoichiometry due to the partial occupation of water molecules expands or contracts the unit cell by ∼2%. Because ettringite phases are important for cement materials and contribute to the overall elastic behavior, we next focused on their elastic properties. For ettringite with 24 water molecules in the stoichiometric formula, we computed the full elastic tensor from which the moduli were derived through standard definitions.[25] Table 2 presents our elastic moduli, together with

Table 2. Theoretical Elastic Properties of Ettringite (in GPa)[a]

property (GPa)	DFT calculations	experiment 2
K	29.96	27.30
G	12.57	9.45
E	33.08	25.95
η	0.32	0.34
$E_{100-010}$	27.95	20.1
E_{001}	55.62	41
anisotropy index	0.505	0.529

[a]The uniaxial Young moduli (E) are given in the [100], [010], and [001] directions corresponding to the a, b, and c lattice parameters, respectively. The experimental data[12] are also included.

the experimental data obtained by Brioullin spectroscopy.[2] The Hill average is presented here. The values obtained for the bulk and shear moduli, as well as the Poisson ratio, agree very well with experiments. The Young's moduli are slightly higher than the experimental values. However, they change systematically in all the directions, preserving the anisotropy of the elastic moduli. Such anisotropy was quantified by the anisotropy index,[26] which represents the difference in elasticity between the crystallographic axes. In ettringite, the elasticity is twice higher in the direction of the columns c than in the perpendicular ones (the a and b plane). Such anisotropy is intimately linked to the water content in ettringite, as we will discuss below.

We turn now to investigate the behavior of ettringite under pressure. Figure 3 shows the lattice parameters and volume against pressure from our calculations, together with the experimental values after X-ray diffraction measurements.[6] The change of the lattice parameters with pressure matches very well with the experiments, with the c axis having a systematic small shift. While in our simulations we reached pressures up to 5 GPa, the experimental data stop at pressures about 1.3 GPa because a quality fit of the lattice parameters was obtainable.[6] Interestingly, a change in slope is found between 2.0 and 3.0 GPa in all the lattice parameters and the volume. The nonlinear evolution for the lattice vectors of ettringite with pressure is coupled with different elastic properties. For instance, if we computed the bulk modulus from the volume versus pressure data in the first slope range for ettringite with 24 water molecules per unit cell, we find a value of 29.7 GPa, in excellent agreement with the 27.8 GPa obtained from the experiments, and the 29.96 GPa from the computed elastic tensor. However, the secondary slope gives an increase of nearly 80% in the bulk modulus, up to 50 GPa. Similar increase takes place for all the studied water contents. Therefore, our simulations reveal a nonlinear response of ettringite crystals to isostatic pressure, independent of the water content, which implies a strengthening of the crystal for pressures larger than 2 GPa.

Experimental studies found a change in the S−O and O−H bond properties at around 2.5 GPa,[6] which might be linked to our discovery of a lattice parameter crossover. We thus analyzed the bonds in more detail by calculating their length distribution d_{O-X} (where X = Ca, Al, S, H) at different pressures. Although all the bond lengths decrease slightly as the pressure increased (up to 0.05 Å), the structure of Ca−O, Al−O, S−O, and H−O bonds was kept under pressure. More interesting is the length distributions of hydrogen bonds $d_{O\cdots H}$. The network of hydrogen bonds for ettringite includes water−water, water−hydroxyl, and water−sulfate bonds, as schematically shown in Figure 4a. At 0.0 GPa, all the hydrogen bonds clearly lie in a range from 1.7 to 2.3 Å with a bimodal distribution, as seen in Figure 4b. When increasing pressure, the first peak maximum in $d_{O\cdots H}$ distances decreased substantially, about 0.2 Å. The second maximum peak, at 2.1 Å, decreases even more noticeably with pressure. In fact, the distances of both peaks became equal at 5.0 GPa. The strength of hydrogen bonds is usually related to their length,[27] as well as the decrease in the accompanying X−H covalent bond strength.[28] Therefore, their interaction becomes stronger under pressure, with a remarkable change after 3 GPa when the water-hydroxyl distance $d_{O\cdots H}$ shrinks even further. This mechanism also explains the increase of the elastic properties. At low pressures, the hydrogen bonds absorb most of the stress by decreasing mainly their bond distances. At higher pressures, the hydrogen bonds interact more closely, with the corresponding increase of the elastic properties of ettringite.

A second parameter that characterizes the network of hydrogen bonds is the OH−O angle. In ettringite, this angle distribution changes with the pressure from a narrow to a wider distribution, indicating that not only do the hydrogen bond distances decrease, but also a reorientation of the water molecules occurs. As shown in Figure 4c, the bond angles at 0.0 GPa have three discrete values: ∼ 4.5°, 9°, and 17°. At high pressures the angles become wider and spread between 5° and 25°. This finding indicates a more disordered hydrogen bond

dx.doi.org/10.1021/jp301822e | J. Phys. Chem. C XXXX, XXX, XXX−XXX

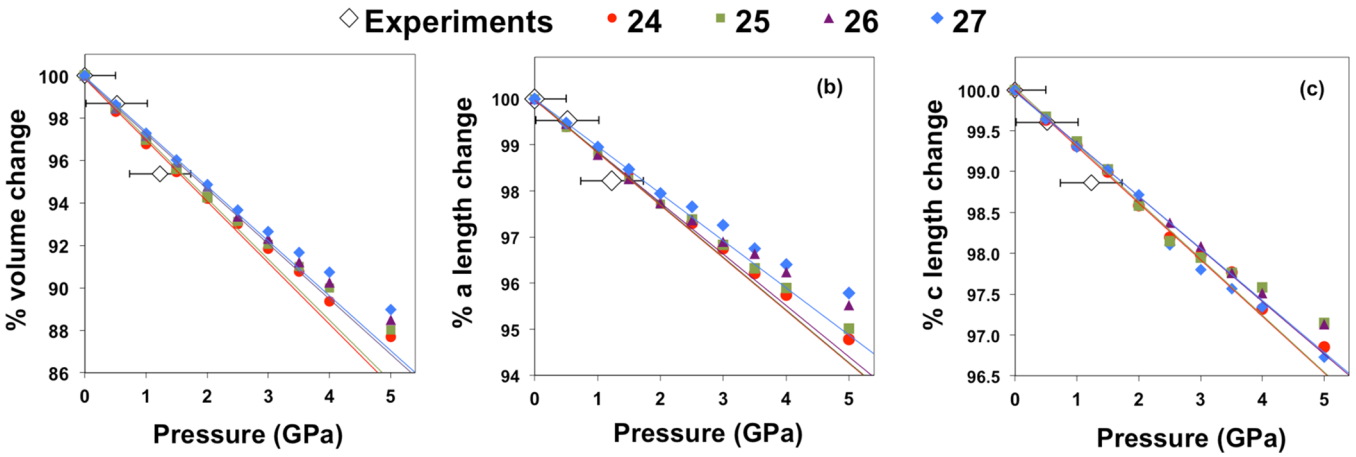

Figure 3. Pressure dependence of the (a) volume and the (b,c) lattice parameters of ettringite with different water occupancies in the unit cell (from 24 to 27). The empty rhombi denote the experimental data from ref 6. Note that the trends are divided into two regions according to the change of slope with pressure. The lines correspond to linear fits of our data at up to 2.0 GPa, and are extended for a better view of the slope change.

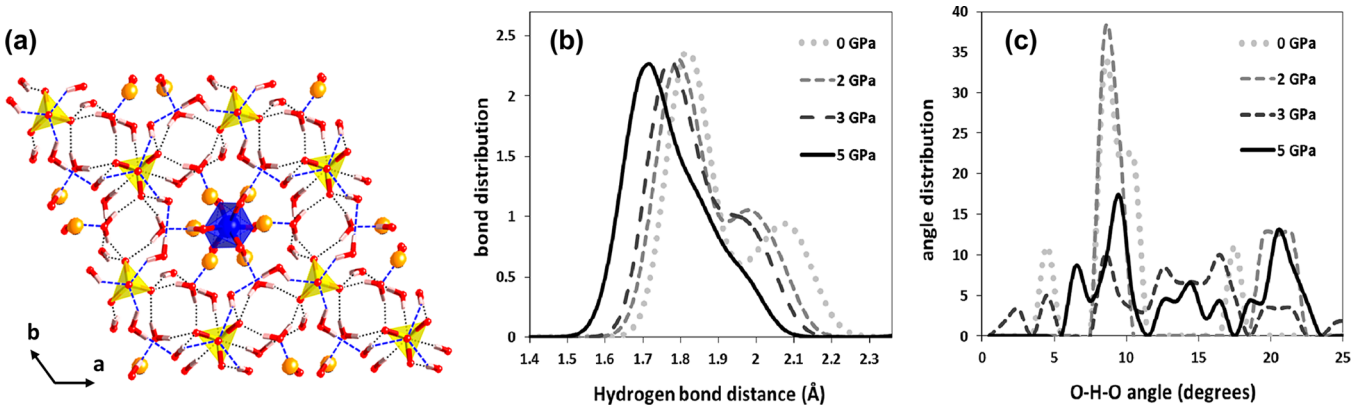

Figure 4. (a) Hydrogen bonded-network structure in ettringite at 0 GPa. Black-dotted and blue-dashed lines represent the hydrogen bonds shorter and larger than 2 Å, respectively. (b) Distance and (c) angle distributions for the hydrogen bonds in ettringite at several pressures.

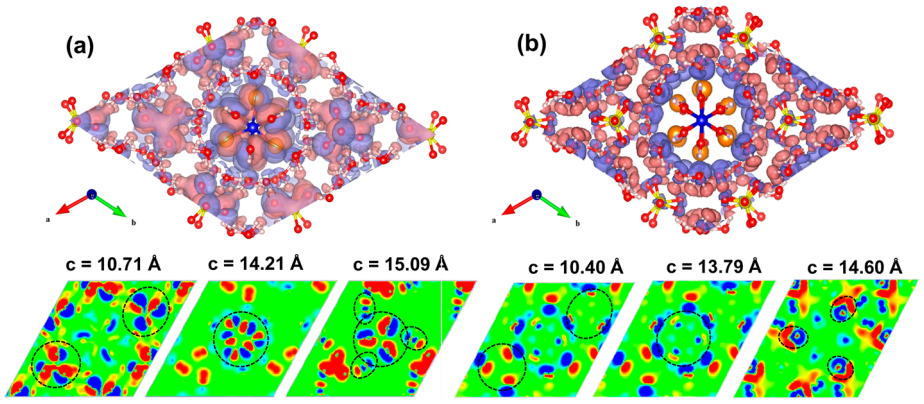

Figure 5. Difference in electronic densities between ettringite with and without water molecules at (a) zero and (b) high (5 GPa) pressures. The unit cell is shifted with respect to Figures 1 and 3 for a better view. Blue and red areas represent excess and defect in electronic density, respectively. Bottom pannels in (a) and (b) are cuts for several *c* values showing the charge polarization of (left) sulfate groups, (middle) hydroxyl groups, and (right) calcium ions and water molecules. For clarity, the mentioned groups are marked by dashed circles.

network, which might be related to the amorphization observed at high pressures in X-ray experiments.[6]

We next analyzed the charge density of ettringite to understand its chemical bonding, looking at the role of water on the cohesion and elastic properties. We have computed the difference in electronic densities between ettringite with and without water. We represented this difference taking $\Delta\rho_{(r)} = \rho_{(r)}(\text{ett}) - \rho_{(r)}(\text{dry}) - \rho_{(r)}(\text{wat})$, where $\rho_{(r)}$ is the electronic density for the unit cell of ettringite, the "dry" means without water, and the "wat" with only water. The difference $\Delta\rho_{(r)}$ is plotted in Figure 5a with the excess and defect electronic density represented with the blue and red areas, respectively. The difference $\Delta\rho_{(r)}$ changes through the entire unit cell, except around the Al atoms that are without polarization. There

dx.doi.org/10.1021/jp301822e | J. Phys. Chem. C XXXX, XXX, XXX–XXX

is a clear charge polarization in the sulfate groups, hydroxyl groups, calcium ions, and water molecules, as seen in the lower panels of Figure 5a. The cohesion between columns in ettringite was previously attributed to a positive charge transfer from the columns to the hydrogen in the water molecules, connected to the negative SO_4^{2-} groups.[8] Rather than charge transfer, the cohesion involves the charge polarizations of columns, water molecules, and sulfate ions.

To understand the changes with pressure, we have also analyzed the difference in electronic density with pressure at 5 GPa, plotted in Figure 5b. It is significant that the maximum value of $\Delta\rho_{(r)}$ decreases with respect to the one at 0 GPa pressure. Only small charge excess is present in sulfate oxygen atoms accompanied with the charge polarization of surrounding water molecules. Compared with panel a, the charge is no longer polarized in the calcium and hydroxyl ions. These changes in $\Delta\rho_{(r)}$ are consistent with a drastic decrease of polarization under pressure. At high pressures, the atoms pack in such a way that their polarizations are negligible. Not only the analysis of the $d_{O\cdots H}$ distances, but also the electronic density distribution confirms the densification of the hydrogen bond network at high pressures.

The crossover of stiffness with pressure is explained by an atomic packing effect. At a zero pressure, the atoms are at their equilibrium distances, and the charge polarization is the dominant interaction. As the pressure increases, the bond distances decrease, entering into the interatomic repulsive regime, a common feature in most crystals. With respect to more homogeneous systems, ettringite includes a diversity of chemical bond types. At low pressures, the hydrogen bonds became shorter without a significant contribution to the repulsive forces, because their potential energy surface is rather flat.[29,30] The crystal then compresses without important repulsive forces in the stiffer iono-covalent bonds. At high pressures, the hydrogen network becomes so packed that their repulsion is comparable to that of the iono-covalent bonds. The whole crystal is now a repulsive system, hence the nonlinear evolution of the volume versus pressure. Because this crossover is related to heterogeneity in the chemical bonds, we expect that this feature is general to crystals with diverse bonding schemes such as layered materials or molecular crystals.[31−33]

There are noteworthy comments on zero point effects. It is well-known that the isotopic substitutions modify the internal vibrations of solids and change the zero-point energy. Ice has shown an anomalous isotope effect with a higher volume for deuterated hexagonal ice with respect to the light one.[34,35] The same effect on zero point vibrations can be reached by increasing either the mass of the isotopes or the pressure. This effect can indeed play a role in the volume changes we found for ettringite at high pressures, and therefore in the increase of the bulk modulus. However, we still lack experimental information about elastic properties or the pressure behavior of deuterated ettringite. Experimental determination of the isotope effect together with a theoretical vibrational analysis will definitely be an interesting topic, although it is beyond the scope of this work.

CONCLUSIONS

Ettringite is a natural mineral with more than half water content. It forms a hydration product in Portland cements and plays a key role in their physical and chemical stability. In this work we have studied its structure, elastic properties, and electronic properties under pressure using simulations within DFT.

We calculated the structure and elastic properties of ettringite with pressure. At a zero pressure, our values agree well with experiments. The elastic moduli are highly anisotropic along different crystallographic directions, such anisotropy is directly related to the nature of the chemical bond in those directions: iono-covalent along the *c* axis, and hydrogen bonding in the *a* and *b* plane. Our calculations indeed show that the charge polarization changes in the ions and molecules between columns, changes that are held responsible for the cohesion in ettringite. At high pressures, above 2.5 GPa, the lattice constants and the crystal elastic properties enter into a different region, where the bulk modulus increases by about 80%. Such drastic change in the elastic properties is related to the densification of the hydrogen bond network. The weak hydrogen bonds compress without inducing big repulsive interatomic forces up to about 2.5 GPa (the crossover pressure), when they become closer, and the oxygen−hydrogen repulsive energy is comparable with the rest of the iono-covalent bonds.

Because the modification of elastic properties with pressure is driven by the heterogeneity of interatomic forces, our results might be generalized to crystals with dissimilar types of chemical bonds, such as molecular crystals, layered materials, etc. These results also point to the importance of hydrogen bonding in the elasticity of crystalline materials, a factor that, to date, has been commonly explored in soft matter such as proteins or polymers.[36,37]

AUTHOR INFORMATION

Corresponding Author

*E-mail: hegoi.manzano@ehu.es.

Notes

The authors declare no competing financial interest.

ACKNOWLEDGMENTS

This study was supported by funding from the Basque Government through the NANOMATERIALS project (Grant No. IE05-151) under the ETORTEK Program (iNanogune), the Spanish Ministerio de Ciencia y Tecnologia of Spain (Grant Nos. TEC2007-68065-C03-03 and Fis2007-66711-C02-02, and MONACEM projects), and the University of the Basque Country (Grant No. IT-366-07). H.M. acknowledges post-doctoral fellowship from the Basque Country Department of Education, Research and Universities. Finally, the computational resources from TeraGrid (TG-DMR110002) and the IZO-SGI, SGIker (UPV/EHU) are acknowledged.

REFERENCES

(1) Anthony, J. W.; Bideaux, R. A.; Bladh, K. W.; Nichols, M. C. *Handbook of Mineralogy*; Mineral Data Publishing: Tuscon, AZ, 2003.
(2) Speziale, S.; Jiang, F. M.; Mao, Z.; Monteiro, P. J. M.; Wenk, H. R.; Duffy, T. S.; Schilling, F. R. *Cem. Concr. Res.* **2008**, *38*, 885.
(3) Hartman, M. R.; Brady, S. K.; Berliner, R.; Conradi, M. S. *J. Solid State Chem.* **2006**, *179*, 1259.
(4) Moore, A. E.; Taylor, H. F. W. *Acta Crystallogr., Sect. B: Struct. Crystallogr. Cryst. Chem.* **1970**, *B 26*, 386.
(5) Goetz-Neunhoeffer, F.; Neubauer, J. *Powder Diffr.* **2006**, *21*, 4.
(6) Clark, S. M.; Colas, B.; Kunz, M.; Speziale, S.; Monteiro, P. J. M. *Cem. Concr. Res.* **2008**, *38*, 19.
(7) Berliner, R. *The Sidney Diamond Symposium: Material Science of Concrete*; American Ceramic Society: Westerville, OH, 1998; p 127.
(8) Moore, A.; Taylor, H. F. W. *Nature* **1968**, *218*, 1048.

(9) Taylor, H. F. *Cement Chemistry*, 2 ed.; Thomas Telford Publishing: London, 1997.
(10) Mehta, P. K.; Monteiro, P. *Concrete: Structure, Properties, and Materials*, 2nd ed.; Prentice Hall: Englewood Cliffs, NJ, 1993.
(11) Taylor, H. F. W.; Famy, C.; Scrivener, K. L. *Cem. Concr. Res.* **2001**, *31*, 683.
(12) Péra, J.; Ambroise, J. *Cem. Concr. Res.* **2004**, *34*, 671.
(13) Chrysochoou, M.; Dermatas, D. *J. Hazard. Mater.* **2006**, *136*, 20.
(14) Zhang, M.; Reardon, E. J. *Environ. Sci. Technol.* **2003**, *37*, 2947.
(15) Albino, V.; Cioffi, R.; Marroccoli, M.; Santoro, L. *J. Hazard. Mater.* **1996**, *51*, 241.
(16) Artacho, E.; Anglada, E.; Dieguez, O.; Gale, J. D.; Garcia, A.; Junquera, J.; Martin, R. M.; Ordejon, P.; Pruneda, J. M.; Sanchez-Portal, D.; Soler, J. M. *J. Phys.: Condens. Matter* **2008**, 20.
(17) Parr, R. G.; Yang, W. *Density-Functional Theory of Atoms and Molecules*; Oxford University Press: Oxford, England, 1989.
(18) Perdew, J. P.; Burke, K.; Ernzerhof, M. *Phys. Rev. Lett.* **1996**, *77*, 3865.
(19) Manzano, H.; Dolado, J. S.; Ayuela, A. *J. Phys. Chem. B* **2009**, *113*, 2832.
(20) Manzano, H.; Dolado, J. S.; Ayuela, A. *J. Am. Ceram. Soc.* **2009**, *92*, 897.
(21) Ayuela, A.; Dolado, J. S.; Campillo, I.; de Miguel, Y. R.; Erkizia, E.; Sanchez-Portal, D.; Rubio, A.; Porro, A.; Echenique, P. M. *J. Chem. Phys.* **2007**, *127*, 164710.
(22) Moreno, J.; Soler, J. M. *Phys. Rev. B* **1992**, *45*, 13891.
(23) Hartman, M. R.; Berliner, R. *Cem. Concr. Res.* **2006**, *36*, 364.
(24) Macrae, C. F.; Edgington, P. R.; McCabe, P.; Pidcock, E.; Shields, G. P.; Taylor, R.; Towler, M.; van De Streek, J. *J. Appl. Crystallogr.* **2006**, *39*, 453.
(25) Manzano, H.; Dolado, J. S.; Ayuela, A. *Acta Mater.* **2009**, *57*, 1666.
(26) Ranganathan, S. I.; Ostoja-Starzewski, M. *Phys. Rev. Lett.* **2008**, 101.
(27) Dougherty, R. C. *J. Chem. Phys.* **1998**, *109*, 7372.
(28) Grabowski, S. J. *J. Phys. Org. Chem.* **2004**, *17*, 18.
(29) Adalsteinsson, H.; Maulitz, A. H.; Bruice, T. C. *J. Am. Chem. Soc.* **1996**, *118*, 7689.
(30) Moilanen, D. E.; Fenn, E. E.; Lin, Y.-S.; Skinner, J. L.; Bagchi, B.; Fayer, M. D. *Proc. Natl. Acad. Sci. U.S.A.* **2008**, *105*, 5295.
(31) Moon, J.; Oh, J. E.; Balonis, M.; Glasser, F. P.; Clark, S. M.; Monteiro, P. J. M. *Cem. Concr. Res.* **2011**, *41*, 571−578.
(32) Elena, V, B. *J. Mol. Struct.* **2003**, *647*, 159.
(33) Yoo, C. S.; Cynn, H.; Gygi, F.; Galli, G.; Iota, V.; Nicol, M.; Carlson, S.; Häusermann, D.; Mailhiot, C. *Phys. Rev. Lett.* **1999**, *83*, 5527.
(34) Rottger, K.; Endriss, A.; Ihringer, J.; Doyle, S.; Kuhs, W. F. *Acta Crystallogr. B* **1994**, *50*, 644.
(35) Herrero, C. P.; Ramirez, R. *J. Chem. Phys.* **2011**, *134*, 094510.
(36) Nair, K. P.; Breedveld, V.; Weck, M. *Soft Matter* **2011**, *7*, 553.
(37) Keten, S.; Xu, Z. P.; Ihle, B.; Buehler, M. J. *Nat. Mater.* **2010**, *9*, 359.